Influence of Solution Chemistry on the Deposition and Detachment Kinetics of a CdTe Quantum Dot Examined using a Quartz Crystal Microbalance

Revised and resubmitted to:
Environmental Science and Technology
February 18, 2009

IVAN R. QUEVEDO and NATHALIE TUFENKJI*

Department of Chemical Engineering
McGill University
Montreal, Quebec
H3A 2B2, Canada

* Corresponding Author. Phone: (514) 398-2999; Fax: (514) 398-6678; E-mail: nathalie.tufenkji@mcgill.ca

Abstract

Recent reports underline the potential environmental and public health risks linked to the "nano" revolution, yet little is known regarding the environmental fate and impacts of most nanomaterials following release in natural soils and groundwaters. Quantum dots (QDs) are one example of engineered nanomaterials that have been demonstrated to exhibit cytotoxic effects; hence the fate of this material in aqueous environments is of particular interest. In this study, a quartz crystal microbalance (QCM) was used to examine the interaction of a commercially available carboxyl terminated CdTe QD with a model sand (i.e., silica) surface. The deposition kinetics of the QD onto clean silica coated QCM crystals were measured over a wide range of solution conditions, in the presence of either monovalent (K^+) or divalent cations (Ca^{2+}). QD deposition rates onto silica were significantly greater in the presence of calcium versus potassium. Solution pH also influenced QD deposition behaviour, with increased deposition observed at a lower pH value. The rate of QD release from the silica surface was also monitored using QCM measurements and found to be comparable to the rate of particle deposition when the monovalent salt was used. In contrast, the rate of QD release was considerably lower from the rate of deposition when particles were deposited in the presence of Ca^{2+}. Physicochemical characterization of the QD suspended in varying electrolytes provided insights into the role of solution chemistry on particle size and electrophoretic mobility (surface charge). Measurements of QD size using dynamic light scattering (DLS) and transmission electron microscopy (TEM) were used to interpret the QD deposition behavior in different solution chemistries. Lower particle deposition rates observed at high ionic strengths were attributed to aggregation of the QDs resulting in decreased convective-diffusive transport to the silica surface.

Introduction

In 2004, about 0.1% of the world's manufactured goods contained nanoparticles, but this is expected to rise to 15% of global output by 2014, with a commercial value of more than $1 trillion (*1*). Massive investment in research and development has led to an amazing array of new products, as evidenced by an exponential increase in the number of patents pending for products and processes involving engineered nanoparticles (*2*). For example, nanoparticles can be used to deliver pharmaceuticals more efficiently, as antibacterial agents in clothing and sanitation equipment, and to store and transmit electronic data on computer chips and microsensors (*3, 4*). Despite the numerous anticipated benefits of nanotechnology, there is great concern that we do not yet fully understand the environmental and health risks associated with this technology.

Quantum dots (QD) are one example of novel engineered nanomaterials that may be used in medical imaging, solar cells, and sensors because of their unique optical and electrical properties (*5-8*). QDs consist of a metalloid crystalline core and a protective shell (e.g., ZnS, CdS) that shields the core and renders the QD bioavailable. The core can consist of a variety of metals that include semiconductors, noble metals, or magnetic transition metals (e.g., CdTe, CdSe). To render QDs biologically compatible or active, they are functionalized with secondary coatings which improve colloidal stability and core durability (*9*). Some researchers have reported that the surface coatings of QDs are subject to photolysis or oxidation (*10, 11*) which may result in dissolution of the core and hence release of toxic metals as hydrated ions. Currently, very little is known regarding the stability of QDs in the environment, product lifetimes, or how these materials partition into environmental media (i.e., air, water, and soil phases). However, it is theorized that the toxicity of QDs depends on their physicochemical properties which may vary under different environmental conditions; namely, particle

size, surface charge, outer coating bioactivity (capping material, functional groups), and oxidative, photolytic, and mechanical stability (*10*). Gagne et al (*12*) have reported the toxicity of CdTe QDs to freshwater mussels. These researchers found that exposure to QDs suspended in aqueous media led to oxidative stress in the gills of the organism and DNA damage in both the gills and digestive glands. Male et al (*13*) found that CdSe QDs exhibited direct cytotoxicity to fibroblasts, whereas CdTe QDs also exhibited indirect toxicity due to release of free cadmium. The introduction of QDs into environmental media may occur via waste streams from industries that synthesize or use QDs and via clinical and research settings. Once released into natural aquatic systems, the potential environmental and health risks associated with QDs will be influenced by their fate and transport within these systems.

The transport and retention of nanomaterials in water saturated granular porous matrices representative of groundwater environments or engineered (deep-bed) granular filtration systems has traditionally been investigated using chromatography columns packed with model granular materials (e.g., glass beads, sand, or soil) (*14-19*). In these bench-scale studies, aqueous suspensions of nanoparticles are injected into columns packed with granular media and particle retention in the granular matrix is commonly interpreted using classical clean-bed filtration theory (*20*). Using this approach, Lecoanet et al (*15*) investigated the transport and deposition behavior of various engineered nanomaterials (fullerols, titanium dioxide, carbon nanotubes, etc) in a water saturated glass bead matrix. These researchers observed considerably differing migration potential for the assorted nanomaterials examined. The transport potential of nanosized zerovalent iron (nZVI) has also been investigated by several researchers (*17, 18, 21, 22*). A number of these laboratory column studies have shown that various types of nZVI, with a wide range of surface modifiers, and sizes ranging from 10 to 200 nm, are transported very efficiently in uncontaminated granular porous media, primarily due to the

stabilizing effect of surface modifiers (*17, 18, 21, 22*). Recent studies have demonstrated how quartz crystal microbalance (QCM) technology can be used to examine the retention and release of nanoparticles onto surfaces in an aqueous environment (*17, 23, 24*). Chen and Elimelech (*23, 24*) used this approach to measure the deposition and detachment of fullerene nanoparticles over a broad range of solution chemistries. They noted that the deposition kinetics of fullerene nanoparticles onto clean silica surfaces are controlled by electrostatic and van der Waals interactions in the presence of monovalent and divalent salts. In contrast, nanoparticle deposition rates were significantly hindered in the presence of humic acid and alginate due to steric stabilization (*24*). Saleh et al (*17*) also used QCM to study the transport and deposition of bare and surface modified nZVI onto a silica coated crystal surface. Their experiments showed how surface modification of the nZVI significantly reduced deposition of the particles onto the silica surface as a result of electrosteric stabilization. In these studies, the silica coated QCM crystal is considered a model collector representing the surface of a sand grain that may be encountered by nanoparticles migrating in a groundwater matrix.

The objective of this work is to examine the deposition and release kinetics of a carboxyl terminated CdTe QD using the QCM. This QD was selected as it is commercially available and representative of functionalized QDs that are stable in aqueous media. Experiments were conducted at two different pHs and a broad range of environmentally relevant solution ionic strengths (IS), examining the influence of both monovalent and divalent cations. Dynamic light scattering (DLS) and transmission electron microscopy (TEM) were used to characterize the size of the QDs at different water chemistries. Particle electrophoretic mobilities (EPMs) were also evaluated.

Materials and Methods

Preparation and Characterization of Quantum Dots. Carboxyl terminated CdTe/CdS QDs with a reported diameter of 10 nm (determined by the manufacturer using transmission electron microscopy) were obtained from Northern Nanotechnologies. QD suspensions at a concentration of 2×10^{13} particles/mL were prepared by diluting the 0.8 μM stock in filtered (0.2 μm nylon filter, Fisher) electrolyte solutions of varying solution chemistry. Analytical reagent-grade KCl and $CaCl_2$ (Fisher) and deionised (DI) water (Biolab) were used to prepare electrolyte solutions. Salt concentrations were varied over a wide range of ionic strengths (1-300 mM) and the pH of the suspensions was adjusted to 5 or 7 by the addition of HCl or KOH (0.1 mM). Prepared QD suspensions were stored at 9°C for 24 hrs prior to each experiment.

The hydrodynamic diameter of the QDs was assessed using dynamic light scattering (DLS) (ZetaSizer Nano, Malvern). Laser Doppler velocimetry (ZetaSizer Nano, Malvern) was used to evaluate QD electrophoretic mobility (EPM). For sizing and EPM measurements, QD suspensions were prepared in the electrolyte solution of interest and each measurement was repeated with at least three different samples. At selected solution conditions, transmission electron microscopy (TEM) was used to confirm the measured size of the particles. Samples were prepared by placing a drop of a QD suspension on a formvar grid, which was left to air dry overnight prior to analysis. Measurements were performed on a Philips CM200 microscope equipped with an AMT CCD camera and operating at 200 kV with a LaB_6 filament.

Quantum Dot Deposition and Release Experiments. QD deposition onto a silica surface was examined using a QCM instrument mounted with silica coated crystals (E4, Q-Sense AB). When the 5 MHz crystals are mounted in the QCM flow modules, the injected flow is parallel to the flat SiO_2

surface (see Figure S1 in Supporting Information). A peristaltic pump (Reglo-Digital IPC-N 4, Ismatec) was used to first inject DI water (100 μL/min) to obtain a stable baseline. Next, the background electrolyte solution of interest was injected into the flow module, followed by a QD suspension in the same electrolyte solution for up to 20 min. The QD suspension was followed by an injection of particle-free electrolyte solution of the same composition. During particle injection into the flow module, deposition of QDs onto the silica surface results in an increase in mass (m) which is recorded as a decrease in the resonance frequency (f) of the quartz crystal. This direct relationship between the resonance frequency of the crystal and the mass adhered to the crystal surface was first reported by Sauerbrey (*25*):

$$\Delta m = -\frac{C}{n}\Delta f_n \tag{1}$$

where n is the overtone (i.e., harmonic) number (1, 3, etc…) and C is the crystal constant (17.7 ng/Hz cm^2). Hence, measurement of variations in the crystal resonance frequency during QD injection provides a means to monitor changes in the mass of deposited QDs with time. The detection limit of the QCM is on the order of ~1 ng/cm^2 which may be limiting when examining low levels of deposition (e.g., when highly repulsive particle-surface interactions predominate). The QD deposition rate (r_d) was evaluated as the rate of change of the frequency shift in a given time period (t), as follows:

$$r_d = \frac{d\Delta f_3}{dt} \tag{2}$$

As shown in eq 2, the QD deposition rate can be determined from the initial slope in the frequency shift measurements. Once a stable deposition rate was observed, the flow was changed to particle free electrolyte at the same ionic strength (to flush the chamber of any undeposited QDs). Next, the chamber was flushed with DI water for 10 min to examine the potential release of QDs from

the silica surface. Hence, the rate of QD release (r_r) is determined from the rate of change of the frequency shift during injection of DI water. QCM experiments were repeated at least three times using suspensions prepared on different days.

Results and Discussion

Size and Zeta Potential of Quantum Dots. To explore the influence of the physicochemical properties of QDs on their deposition behavior, the QD electrophoretic mobility (EPM) and size were evaluated as a function of the electrolyte species and concentration. The QD EPM is negative over the entire range of solution chemistries examined (Figure 1). This negative surface charge can be attributed to the presence of carboxyl functional groups in the shell coating of the QDs. The particles generally become less negative with increasing concentration of either KCl or $CaCl_2$ as a result of compression of the diffuse double-layer of ions at the particle surface. Inspection of Figure 1 reveals large error bars in the reported QD EPMs. These large variations in the measurements suggest that the QD suspensions are not fully stabilized and monodispersed. In the presence of the monovalent salt (KCl), the QD EPM was less negative at lower pH with values ranging between -2.4 to -2.1 μmcm/Vsec at pH 5, while at pH 7, the EPM varied between -3.1 to -2.5 μmcm/Vsec (Fig. 1a). If the Smoluchowski equation is used to evaluate the QD zeta potentials from the EPMs, they are found to range from -40 to -45 mV in KCl at pH 7 and between -30 to -35 mV in KCl at pH 5 (*26*). The results obtained in Figure 1 are in general agreement with those reported by Zhang et al. (*27*), where they observed a decrease in the absolute zeta potential of thioglycolate functionalized QDs with increasing IS. The QD EPM measured in KCl at pH 7 has a lower absolute value than that of carboxyl-modified latex nanospheres under similar conditions (*28, 29*). Behrens et al (*28*) reported EPMs on the order of -4 μmcm/Vsec for 52 nm latex particles suspended in KCl at pH 7, whereas Tufenkji and Elimelech reported a zeta potential of -50 to -58.5 mV for 63 nm carboxyl-modified latex particles suspended in

KCl at pH 8 (*29*). In the presence of the divalent cation (Ca^{2+}), we noted a significant decrease in the absolute value of the QD EPM, with absolute values ranging between -1.8 and -1.5 μmcm/Vsec (Fig. 1b). These findings are also in agreement with the measurements of Zhang et al. (*27*) obtained in the presence of the divalent ions Mg^{2+} and Ca^{2+}.

[FIGURE_1_HERE]

The mean diameters and particle size distributions of the QDs were studied over a broad range of ionic strengths at two different pHs using DLS (Figure 2). In general, the size of the QDs increased with electrolyte concentration. This was particularly clear at pH 5 in both salts. When the QDs are suspended in KCl (pH 5), the hydrodynamic diameter is between 45 and 100 nm below 155 mM IS but demonstrates considerable instability above this IS (i.e., the error bars for these measurements are quite large) (Figure 2a). At pH 7, the particle size measured by DLS remains in the same range (45 to 100 nm) below 100 mM but again becomes more unstable at higher IS (Figure 2a). When the QDs are suspended in a $CaCl_2$ solution, marked aggregation is observed with increasing salt concentration (Figure 2b). In the presence of $CaCl_2$, the critical coagulation concentration (CCC) is much lower (12 mM) than that observed for the monovalent salt (~155 mM) (note: in this discussion, the CCC is estimated from the data presented in Figure 2). Because the scattering intensity of the particles is roughly proportional to d^6 (Rayleigh approximation), DLS measurements are strongly influenced by the presence of aggregates. Hence, the values reported in Figure 2 are expected to be larger than those assessed with microscopic techniques such as transmission electron microscopy (TEM). In Figure 3a, a TEM image of a QD sample suspended in 15 mM KCl reveals the presence of irregularly shaped QDs on the order of 10 to 20 nm. On the other hand, when the QDs are suspended in 12 mM $CaCl_2$ (Figure 3b), the particles tend to aggregate in irregular clusters of more than 100 nm in size. These

results are consistent with those reported by Zhang et al. (*27*) where considerable aggregation of QDs was observed in the presence of calcium, even with a relatively low concentration of the divalent cation.

[FIGURE_2_HERE]

[FIGURE_3_HERE]

A comparison of particle size distributions of selected samples determined by DLS are shown in Figure 2c and 2d. At lower ionic strength (15 mM), the particle size distribution resembles a lognormal distribution, while at higher salt concentration (255 mM) the QD suspension exhibits a broader size distribution. At the higher IS examined (above the CCC), the particle suspension is very unstable and the DLS technique captures a bimodal distribution in the particle size.

Deposition of Quantum Dots onto a Silica Surface. Figure S2a shows representative QCM measurements (frequency shifts) for an experiment where the QDs are suspended in KCl at pH 5. In step A, DI water is injected to achieve a stable baseline (constant frequency) followed by 205 mM KCl (pH 5), whereas in step B a suspension containing QDs with the same concentration of salt and pH is injected into the QCM flow chamber. Because the measured frequency shift is proportional to the amount of mass on the silica surface, the QD deposition rate onto the clean silica surface is determined by calculating the initial slope of the measured frequency shifts as a function of time (as described in eq 2). Figure S2b shows representative measurements of the frequency shift from QD deposition experiments at different solution IS (KCl, pH 5). As the solution IS increases, we note an increase in the slope of the frequency shift, and hence, an increase in the QD deposition rate, r_d (based on eq 2). Values of the deposition rate determined from experiments conducted over a broad range of solution

IS at two different pHs are presented in Figure 4. In this figure, the data are presented in terms of ng/min where the mass of deposited nanoparticles was evaluated using the Sauerbrey relation (eq 1).

[FIGURE_4_HERE]

At pH 5 (open squares in Figure 4a), the QD deposition rate increases significantly with increasing IS up to 155 mM KCl. The observed increase in the QD deposition rate with increasing salt concentration is in qualitative agreement with other studies of nanoparticle retention conducted under conditions deemed unfavorable for deposition (*14, 24, 29, 30*). Namely, when the nanoparticles and collector surfaces (e.g., glass beads or silica surfaces) are both negatively charged, an increase in solution IS results in a decrease in the range and magnitude of repulsive electrostatic interactions, and hence, a decrease in deposition.

When the solution IS exceeds 155 mM (at pH 5), the measured QD deposition rate decreases (Figure 4a). This behavior can be attributed to a loss in stability of the QD suspension at high salt concentrations. The sizing data reported in Figure 2 show that the average diameter of the QDs increases at high solution IS and the DLS measurements are more unstable (larger error bars) under these conditions. The data in Figure 2 suggest that the CCC of the QDs is between 155 and 200 mM at pH 5. The larger QD aggregates formed at high IS have a significantly lower diffusion coefficient than the stable QDs and hence will experience lowered convective-diffusive transport to the silica-coated surface. Similar behavior was observed by Chen and Elimelech for the deposition of fullerene nanoparticles onto bare or humic coated silica surfaces (*23, 24*).

The results of QCM experiments conducted at pH 7 are presented in Figure 4b as solid symbols. At this higher pH, the QD deposition rate is near zero over the entire range of IS examined.

These results contrast with the data obtained at pH 5 where significantly higher QD deposition rates were measured. At pH 7, the QDs exhibit a more negative zeta potential (Figure 1), and the silica surface is also more negatively charged (*31*). This greater absolute potential of the like-charged surfaces gives rise to more significant repulsive electrical double-layer interactions upon approach of the QDs to the silica surface. Hence, the results shown in Figure 4b suggest that, even at high solution IS, the carboxyl-terminated QDs are not expected to be effectively retained on sand surfaces at neutral pH in the presence of the monovalent KCl salt.

To examine the influence of a divalent cation on QD deposition kinetics, QCM experiments were conducted with QDs suspended in a $CaCl_2$ solution at pH 5 (Figure 4c). Comparison of the results obtained in Figure 4a and 4c shows that the QD deposition rate is significantly higher in the presence of the divalent cation versus the monovalent cation. In the case of $CaCl_2$, the QD deposition rate (r_d) increases with increasing salt concentration up to an IS of 12 mM. Above this critical concentration, the QD deposition rate onto the silica surface exhibits more instability and tends to decrease. This behaviour can again be explained by considering the stability of the QD suspension over the range of salt concentrations examined. At ionic strengths below 12 mM, the QDs are relatively stable (Figure 2b), however above this CCC, the QDs tend to form larger aggregates (Figure 3b) and will therefore experience lessened convective-diffusive transport to the silica surface. Hence, even though the QD electrophoretic mobility (and hence zeta potential) becomes less negative with increasing concentration of $CaCl_2$ (Figure 1c), the QD deposition rate decreases above the CCC due to the formation of aggregates. It is interesting to note that the QD CCC in $CaCl_2$ is considerably lower (12 mM) than in the monovalent salt (155 mM).

To confirm the proposed hypothesis that the measured QD deposition rates decrease at high solution IS due to QD aggregation and a corresponding decrease in convective-diffusive transport, the

experimental data in Figure 4 can be compared to the theoretical particle deposition rates. The theoretical particle deposition rate (r_d^{SL}) in the absence of electrostatic interactions can be evaluated using the Smoluchowski-Levich approximation for parallel-plate geometry which is a valid approximation for the E4 QCM flow chamber (*32*):

$$r_d^{SL} = 0.538 \frac{D_\infty C_b}{a_p} \left(\frac{Pe \cdot h}{x} \right)^{1/3} \quad (3)$$

where D_∞ is the diffusion coefficient, C_b is the bulk concentration of QDs, a_p is the radius of the QDs based on DLS measurements (Fig. 2), Pe is the dimensionless particle Péclet number, h is the height of the QCM flow chamber, and x is the distance along the flow from the inlet.

Equation 3 was used to calculate the theoretical QD deposition rates and the results are compared to the experimental measurements in Figure 4. At low solution IS where repulsive electrostatic interactions predominate, QD deposition rates measured in KCl at pH 5 are significantly lower than r_d^{SL}. As the IS increases, the experimental rates approach values of r_d^{SL}. As noted above, when the KCl concentration exceeds 155 mM, the measured QD deposition rates decrease with increasing solution IS (Fig 4a). A similar trend is noted for the theoretical particle deposition rates represented by the open stars. In Figure 4b, the QD deposition rates measured in KCl at pH 7 are significantly lower than r_d^{SL} over the entire range of IS examined. This difference between theoretical and experimental deposition rates is caused by the presence of strong repulsive electrostatic interactions at the higher pH. Similar behavior is noted for experiments conducted at low solution IS with QDs suspended in $CaCl_2$ (Fig. 4c); namely, values of r_d^{SL} are much greater than the experimental rates under conditions deemed unfavorable for deposition. In contrast, when the IS of the $CaCl_2$ solution is increased above 8 mM, experimental QD deposition rates are nearly equivalent to r_d^{SL} (Fig. 4c). In

summary, the results shown in Figure 4 reveal that for all three cases, the theoretical particle deposition rate (represented by open stars in Fig. 4a, b, c) decreases over the range of IS as a result of particle aggregation and a corresponding decrease in convective-diffusive transport.

Release Kinetics of Quantum Dots. In the natural subsurface environment, changes in solution chemistry might cause release of colloids from soil surfaces. For instance, a rainfall can result in significant decreases in water IS, potentially causing detachment of particles from the soil grain surfaces (*33*). To better understand the reversibility of QD retention on the silica surface, a series of release experiments were conducted whereby the QCM chamber was rinsed with DI water at the same flowrate used during nanoparticle injection. Representative QCM measurements during the injection of DI water are shown in Figure S2a (phase D). In these experiments, the QD release rate (r_r) can be determined by calculating the slope of the frequency shift during injection of DI water. Calculated values of r_r are compared to calculated values of r_d in Figure 5a and Figure 5b for experiments conducted in KCl (pH 5) or $CaCl_2$ (pH 5), respectively. Figure 5a shows that for QDs deposited in the presence of KCl, the rate of QD release from the silica surface was nearly equal to the rate of QD deposition over the range of IS examined. In contrast, when QDs were deposited in the presence of $CaCl_2$ (Figure 5b), the rate of QD release (r_r) is low in comparison to the rate of QD deposition (r_d). In fact, the values of r_r are near zero over the range of $CaCl_2$ concentrations, except near the CCC. The higher rate of QD release at the CCC may be caused by the breakup and/or release of weakly formed QD aggregates.

The fraction of QDs released during injection of DI water was calculated from the measured frequency shifts and is plotted in Figure S3. These calculations show that a small fraction of QDs is released when the particles are deposited at a relatively low IS (below the CCC); namely, the fraction

released is less than ~20% in KCl, and less than ~10% in $CaCl_2$. On the other hand, the fraction of QDs released is greater when particles are deposited at IS above the CCC. This finding is counter-intuitive in that particles deposited in the presence of the divalent cation are expected to be irreversibly attached, particularly when deposited at higher salt concentrations (*34*). Hence, this result further supports the hypothesis that the higher release rate (and fraction of particles released) observed at the CCC (12 mM) in $CaCl_2$ can be attributed to breakup and/or release of weakly formed QD aggregates. This would also explain the greater release of particles noted for the experiments conducted in high IS KCl (Figure S3a).

[FIGURE_5_HERE]

Environmental Implications

Following the release of quantum dots in the natural environment, their potential risks to ecosystems and public health will be governed by their transport and fate. The data reported in this study begins to fill the knowledge gaps regarding the physicochemical properties and transport potential of one type of manufactured QD in aqueous media. Northern Nanotechnologies sells this material for a wide range of applications, including fluorescence-based biological sensing and solar devices. In the presence of a monovalent cation, the selected QD is shown to be relatively stable at low solution IS, but significant aggregation is observed at higher IS (above 155 mM). The QDs aggregate at much lower solution IS (12 mM) in the presence of a divalent cation. EPM measurements are challenging with this nanoscale system that tends to aggregate, but reveal observable variations with water chemistry. At pH 5, the extent of QD deposition increases with IS until it reaches the CCC. Above this salt concentration, the QD deposition rate decreases due to decreased convective-diffusive transport to the silica surface. Very little QD deposition is observed at neutral pH suggesting that the transport potential of this

nanomaterial is significant at pH 7. The rate of particle detachment from the silica surface is quite important at pH 5, suggesting that additional investigations examining the potential re-mobilization of QDs upon changes in water chemistry are needed to better understand the contamination risks associated with this nanomaterial.

Complementary studies conducted using laboratory-scale packed columns will provide additional insights into the migration behavior of QDs in water saturated granular systems. Natural groundwater can contain a wide range of components, including dissolved organic matter, biological exudates, and biocolloids. Continuing research in our laboratory aims at extending this work to examine the transport of QDs in aquatic environments over a wider range of environmentally relevant conditions. Moreover, preliminary experiments in our laboratory illustrate the varying behavior of QDs composed of different core materials and having different surface functionalizations. Many commercial QDs are CdSe/ZnS based, whereas the product used in this study is CdTe/CdS based. Hence, additional studies are needed to better characterize the transport potential of these engineered nanomaterials on a case-by-case basis.

Acknowledgements

The authors acknowledge the financial support of the Fonds québécois de la recherche sur la nature et les technologies (FQRNT Team Grant and New Researchers Grant), Roberto Rocca Foundation, and CONACYT for fellowships awarded to I.R.Q.

Literature Cited

1. Lux Research Inc., *The Nanotech Report, 4th ed.,* 2004.
2. Roco, M. C., Broader societal issues of nanotechnology. *J. Nanoparticle Res.* **2003,** *5*, 181-189.
3. Somorjai, G. A.; McCrea, K., Roadmap for catalysis science in the 21st century: a personal view of building the future on past and present accomplishments. *Appl. Catalysis A: General* **2001,** *222*, 3-18.
4. McNeil, S. E., Nanotechnology for the biologist. *J. Leukocyte Biol.* **2005,** *78*, 585-594.
5. Posani, K. T.; Tripathi, V.; Annamalai, S.; Weisse-Bernstein, N. R.; Krishna, S.; Perahia, R.; Crisafulli, O.; Painter, O. J., Nanoscale quantum dot infrared sensors with photonic crystal cavity. *Applied Physics Letters* **2006,** *88*, 151104.
6. Nozik, A. J., Quantum dot solar cells. *Physica E* **2002,** *14*, 115-120.
7. Gao, X.; Cui, Y.; Levenson, R. M.; Chung, L. W. K.; Nie, S., *In vivo* cancer targeting and imaging with semiconductor quantum dots. *Nature Biotechnology* **2004,** *22*, (8), 969-976.
8. Alivisatos, A. P., The use of nanocrystals in biological detection. *Nature Biotechnology* **2004,** *22*, (1), 47-52.
9. Dabbousi, B. O.; Rodriguez-Viejo, J.; Mikulec, F. V.; Heine, J. R.; Mattoussi, H.; Ober, R.; Jensen, K. F.; Bawendi, M. G., (CdSe)ZnS core-shell quantum dots: Synthesis and characterization of a size series of highly luminescent nanocrystallites. *Journal of Physical Chemistry B* **1997,** *101*, (46), 9463-9475.
10. Hardman, R., A toxicological review of quantum dots: toxicity depends on physicochemical and environmental factors. *Environ. Health Perspec.* **2006,** *114*, (2), 165-172.
11. Aldana, J.; Wang, Y. A.; Peng, X., Photochemical instability of CdSe nanocrystals coated by hydrophilic thiols. *Journal of the American Chemical Society* **2001,** *123*, (36), 8844-8850.
12. Gagne, F.; Auclair, J.; Turcotte, P.; Fournier, M.; Gagnon, C.; Sauve, S.; Blaise, C., Ecotoxicity of CdTe quantum dots to freshwater mussels: Impacts on immune system, oxidative stress and genotoxicity. *Aquatic Toxicology* **2008,** *86*, 333-340.
13. Male, K. B.; Lachance, B.; Hrapovic, S.; Sunahara, G.; Luong, J. H. T., Assessment of Cytotoxicity of Quantum Dots and Gold Nanoparticles Using Cell-Based Impedance Spectroscopy. *Analytical Chemistry* **2008,** *80*, (14), 5487-5493.
14. Pelley, A. J.; Tufenkji, N., Effect of particle size and natural organic matter on the migration of nano- and microscale latex particles in saturated porous media *Journal of Colloid and Interface Science* **2008,** *321*, 74-83.
15. Lecoanet, H. F.; Bottero, J.-Y.; Wiesner, M. R., Laboratory Assessment of the Mobility of Nanomaterials in Porous Media. *Environ. Sci. Technol.* **2004,** *38*, 5164-5169.
16. Lecoanet, H. F.; Wiesner, M. R., Velocity Effects on Fullerene and Oxide Nanoparticle Deposition in Porous Media. *Environ. Sci. Technol.* **2004,** *38*, 4377-4382.
17. Saleh, N.; Sirk, K.; Liu, Y.-Q.; Phenrat, T.; Dufour, B.; Matyjaszewski, K.; Tilton, R. D.; Lowry, G. V., Surface modifications enhance nanoiron transport and NAPL targeting in saturated porous media. *Environ. Eng. Sci.* **2007,** *24*, (1), 45-57.
18. Kanel, S. R.; Nepal, D.; Manning, B.; Choi, H., Transport of surface-modified iron nanoparticle in porous media and application to arsenic(III) remediation. *Journal of Nanoparticle Research* **2007,** *9*, 725-735.
19. Franchi, A.; O'Melia, C. R., Effects of Natural Organic Matter and Solution Chemistry on the Deposition and Reentrainment of Colloids in Porous Media. *Environ. Sci. Technol.* **2003,** *37*, 1122-1129.
20. Yao, K. M.; Habibian, M. T.; O'Melia, C. R., Water and Waste Water Filtration - Concepts and Applications. *Environ. Sci. Technol.* **1971,** *5*, (11), 1105-1112.
21. He, F.; Zhao, D.; Liu, J.; Roberts, C. B., Stabilization of Fe-Pd Nanoparticles with Sodium Carboxymethyl Cellulose for Enhanced Transport and Dechlorination of Trichloroethylene in Soil and Groundwater. *Ind. Eng. Chem. Res.* **2007,** *46*, 29-34.
22. Saleh, N.; Kim, H.-J.; Phenrat, T.; Matyjaszewski, K.; Tilton, R. D.; Lowry, G. V., Ionic Strength and Composition Affect the Mobility of Surface-Modified Fe0 Nanoparticles in Water-Saturated Sand Columns. *Environ. Sci. Technol.* **2008,** *42*, 3349-3355.
23. Chen, K. L.; Elimelech, M., Aggregation and Deposition Kinetics of Fullerene (C60) Nanoparticles. *Langmuir* **2006,** *22*, 10994-11001.
24. Chen, K. L.; Elimelech, M., Interaction of Fullerene (C60) Nanoparticles with Humic Acid and Alginate Coated Silica Surfaces: Measurements, Mechanisms and Environmental Implications *Environ. Sci. Technol.* **2008,** *42*, 7607-7614.

25. Sauerbrey, G., Verwendung von Schwingquarzen zur Wagung dunner Schichten und zur Mikrowagung. *Zeitschrift fiir Physik* **1959,** *155*, 206-222.
26. Hunter, R. J., *Foundations of Colloid Science*. Oxford University Press: New York, 2001; p 806.
27. Zhang, Y.; Chen, Y.; Westerhoff, P.; Crittenden, J. C., Stability and removal of water soluble CdTe quantum dots in water. *Environ. Sci.Technol.* **2008,** *42*, (1), 321-325.
28. Behrens, S. H.; Christl, D. I.; Emmerzael, R.; Schurtenberger, P.; Borkovec, M., Charging and Aggregation Properties of Carboxyl Latex Particles: Experiments versus DLVO Theory. *Langmuir* **2000,** *16*, 2566-2575.
29. Tufenkji, N.; Elimelech, M., Breakdown of Colloid Filtration Theory: Role of Secondary Energy Minimum and Surface Charge Heterogeneities. *Langmuir* **2005,** *21*, 841-852.
30. Espinasse, B.; Hotze, E. M.; Wiesner, M. R., Transport and Retention of Colloidal Aggregates of C60 in Porous Media: Effects of Organic Macromolecules, Ionic Composition, and Preparation Method. *Environ. Sci.Technol.* **2007,** *41*, 7396-7402.
31. Bergna, H. E.; Roberts, W. O.; Editors, *Colloidal Silica: Fundamentals and Applications*. 2006; p 912 pp.
32. Adamczyk, Z.; van de Ven, T. G. M., Deposition of Particles under External Forces in Laminar Flow through Parallel-Plate and Cylindrical Channels. *Journal of Colloid and Interface Science* **1981,** *80*, (2), 340-356.
33. Ryan, J. N.; Elimelech, M., Colloid mobilization and transport in groundwater. *Colloids and Surfaces A: Physicochem. Eng. Aspects* **1996,** *107*, 1-56.
34. Hahn, M. W.; Abadzic, D.; O'Melia, C. R., Aquasols: On the Role of Secondary Minima. *Environmental Science & Technology* **2004,** *38*, 5915-5924.

Figure Captions

FIGURE 1. Electrophoretic mobility of quantum dots suspended in different electrolytes: (a) KCl (pH 5 and 7), (b) $CaCl_2$ (pH 5). Data represent the mean ± 95% confidence interval.

FIGURE 2. Average hydrodynamic diameter of QDs determined by dynamic light scattering (DLS) when suspended in (a) KCl and (b) $CaCl_2$. Data represent the mean ± 95% confidence interval. Quantum dot particle size distributions at pH 5: (c) 15 mM KCl, and (d) 255 mM KCl.

FIGURE 3. TEM images of quantum dots prepared in the following electrolytes: (a) 15 mM KCl, (b) 12 mM $CaCl_2$.

FIGURE 4. Comparison of experimental values of the QD deposition rate (r_d) determined using eq 2 and theoretical rates (✯) determined using the Smoluchowski-Levich approximation for a parallel-plate flow chamber (eq 3) and the measured particle sizes from Fig. 2 for QDs suspended in (a) KCl solution at pH 5; (b) KCl solution at pH 7; and (c) $CaCl_2$ at pH 5. Data represent the mean ± 95% confidence interval.

FIGURE 5. Calculated values of the QD deposition (r_d) and release (r_r) rates for QDs suspended in (a) KCl solution and (b) $CaCl_2$ at pH 5. Data represent the mean ± 95% confidence interval.

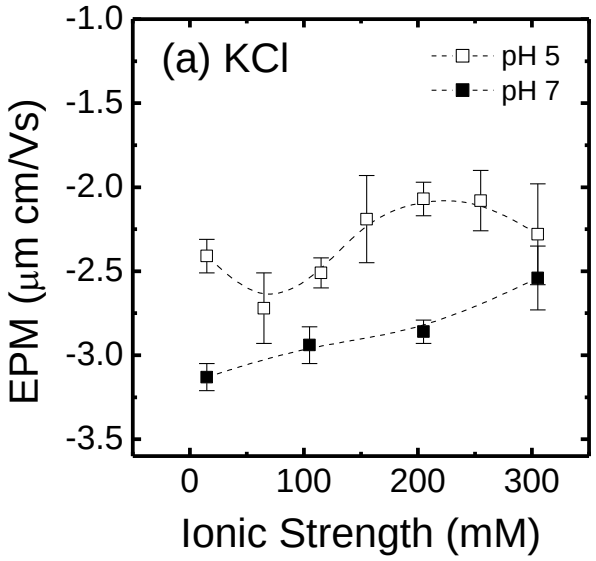

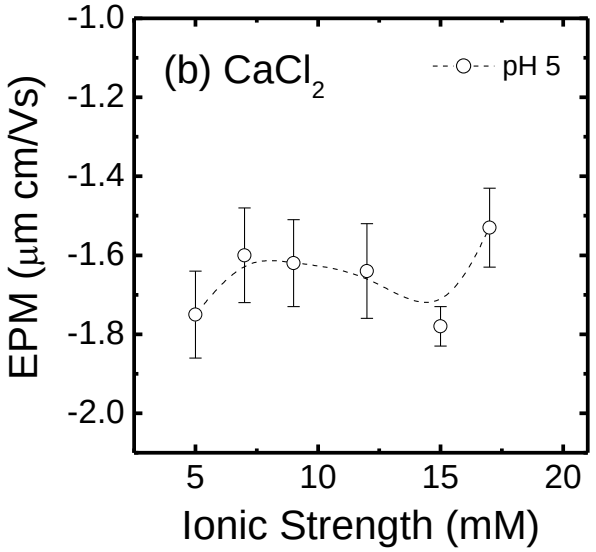

Quevedo and Tufenkji

FIGURE 1

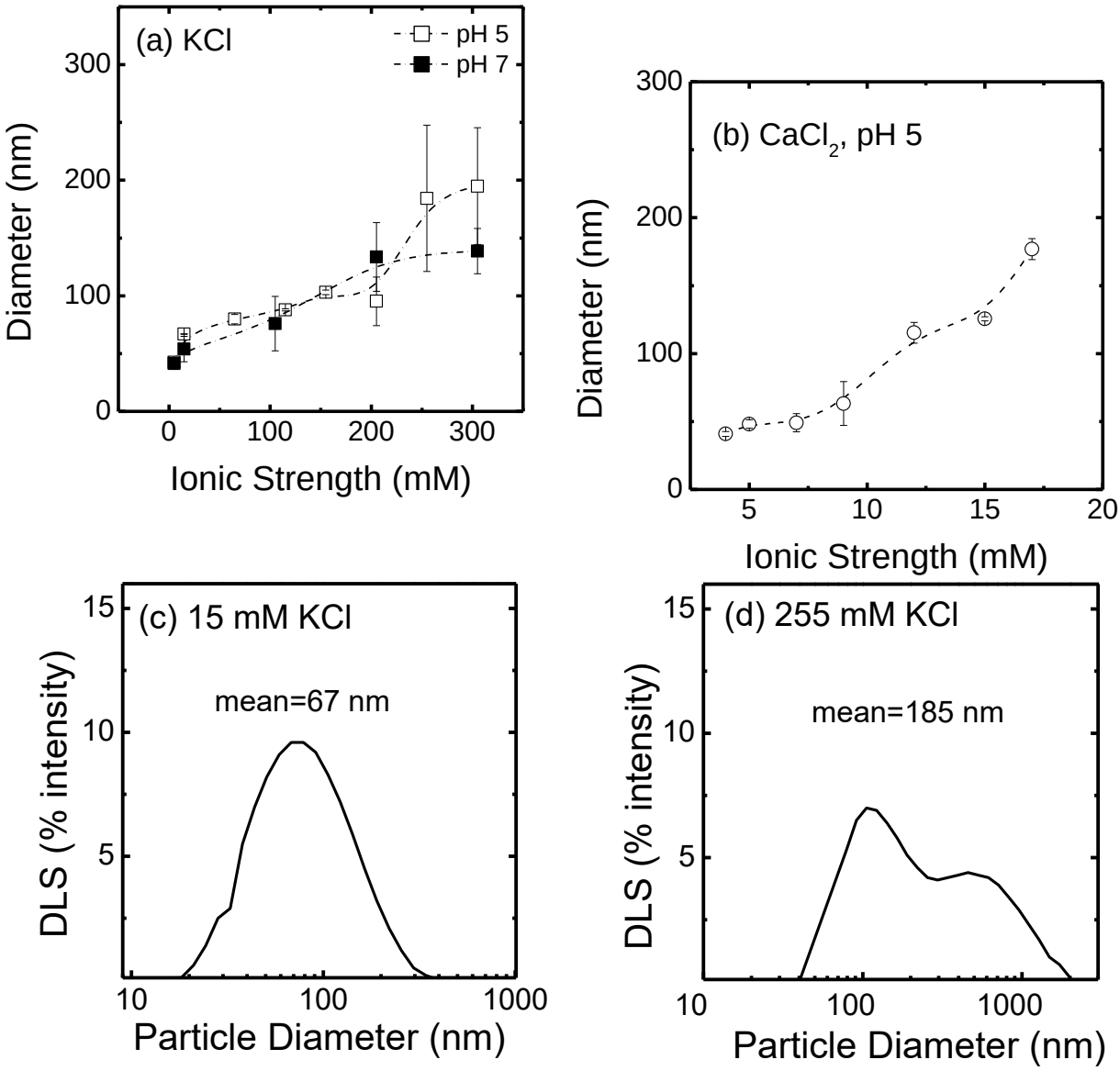

Quevedo and Tufenkji

FIGURE 2

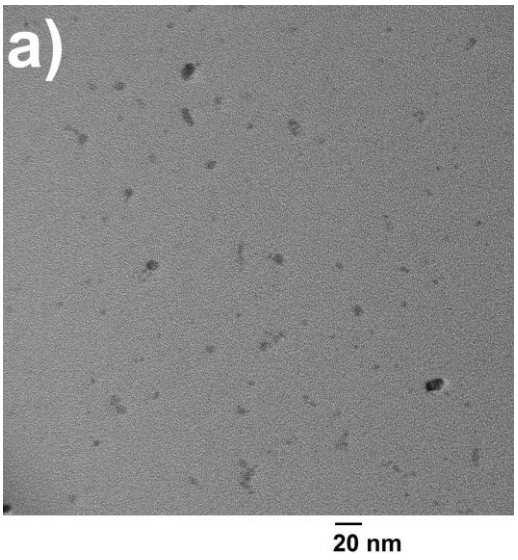

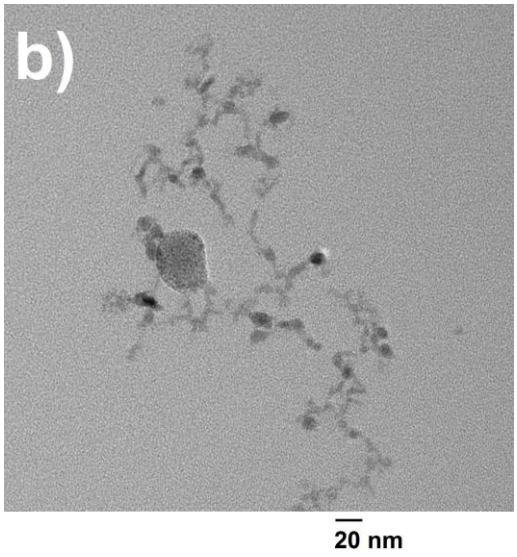

Quevedo and Tufenkji

FIGURE 3

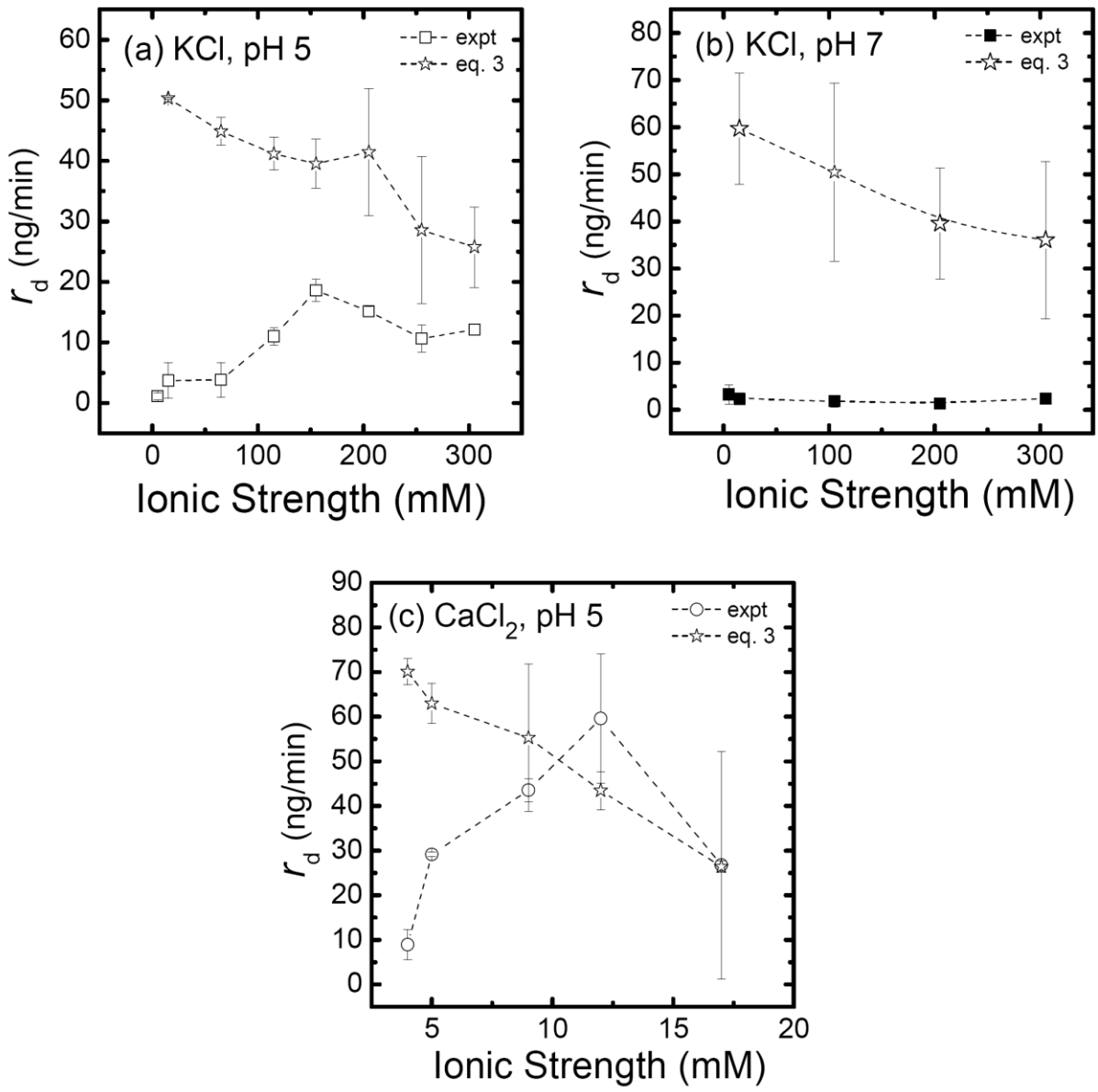

Quevedo and Tufenkji

FIGURE 4

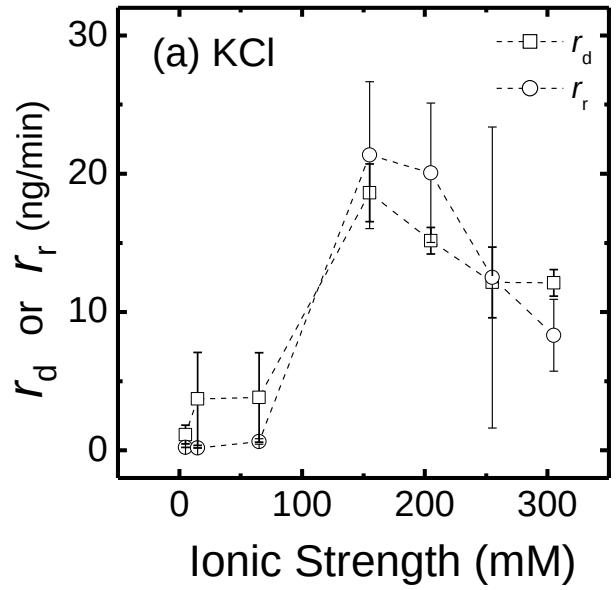

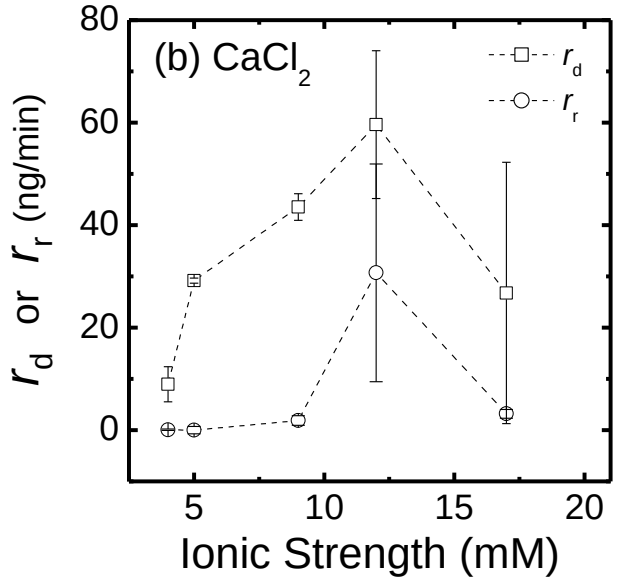

Quevedo and Tufenkji

FIGURE 5

BRIEF

A quartz crystal microbalance is used to monitor the influence of solution chemistry on the transport and retention of CdTe quantum dots on a silica surface.